nature neuroscience

AGRP neurons are sufficient to orchestrate feeding behavior rapidly and without training

Yexica Aponte, Deniz Atasoy & Scott M Sternson

Two intermingled hypothalamic neuron populations specified by expression of agouti-related peptide (AGRP) or pro-opiomelanocortin (POMC) positively and negatively influence feeding behavior, respectively, possibly by reciprocally regulating downstream melanocortin receptors. However, the sufficiency of these neurons to control behavior and the relationship of their activity to the magnitude and dynamics of feeding are unknown. To measure this, we used channelrhodopsin-2 for cell type–specific photostimulation. Activation of only 800 AGRP neurons in mice evoked voracious feeding within minutes. The behavioral response increased with photoexcitable neuron number, photostimulation frequency and stimulus duration. Conversely, POMC neuron stimulation reduced food intake and body weight, which required melanocortin receptor signaling. However, AGRP neuron–mediated feeding was not dependent on suppressing this melanocortin pathway, indicating that AGRP neurons directly engage feeding circuits. Furthermore, feeding was evoked selectively over drinking without training or prior photostimulus exposure, which suggests that AGRP neurons serve a dedicated role coordinating this complex behavior.

Multiple neuron populations distributed throughout the brain influence the decision to seek and consume food[1]. AGRP neurons are thought to positively regulate feeding behavior because AGRP[2] and a coexpressed peptide, neuropeptide Y (NPY)[3–5], increase food intake when injected into the brain. Moreover, the firing rate of AGRP neurons is elevated in brain slices from food-deprived mice[6]. In contrast, genetic and pharmacologic evidence suggest that POMC neurons inhibit feeding by releasing α-melanocyte–stimulating hormone, a melanocortin receptor agonist[7,8]. Both of these populations are located in the hypothalamic arcuate nucleus (ARC). In the ARC, AGRP neurons inhibit POMC neurons[9,10]. In addition, AGRP directly blocks melanocortin receptors[2]. Thus, AGRP neurons have been proposed to serve a modulatory function, counter-regulating the melanocortin pathway to reduce satiety and promote food intake[11].

However, loss-of-function experiments, which showed that AGRP neuron ablation in adult mice leads to anorexia[12], can not be explained by disinhibition of melanocortin signaling[13]. Instead, starvation was proposed to result from severe gastrointestinal malaise[14], and food intake could be permanently rescued by benzodiazepine treatment[14]. Thus, it is unclear whether AGRP neurons directly control feeding or if their role is instead permissive, either preventing a state of intense nausea or suppressing melanocortin signaling. This distinction raises the question of whether AGRP neuron activity is sufficient to evoke feeding behavior and, if so, whether suppression of melanocortin signaling is required for this. To address these issues, we sought to directly determine the role of these neurons for feeding by rapidly and cell type–selectively increasing their electrical activity.

RESULTS

Cell type–specific neuron activation

To overcome cell-type heterogeneity in the ARC, which contains AGRP and POMC neurons and several other cell populations, we used light to selectively stimulate either AGRP or POMC neurons. The light-activated cation channel channelrhodopsin-2 (ChR2)[15,16], fused to the fluorophore tdtomato (ChR2:tdtomato), was targeted to AGRP or POMC neurons by injecting the Cre recombinase–dependent viral vector rAAV-FLEX-*rev*-ChR2:tdtomato[17] into the ARC of *agrp-cre*[18] and *pomc-cre*[19] transgenic mice, rendering these neurons photoexcitable. The cell-type selectivity of this viral approach and the ChR2-dependent photoexcitability of these cell populations have been demonstrated previously[17].

For light delivery, an optical fiber was targeted to the dorsal portion of the hypothalamus in mice expressing ChR2:tdtomato in AGRP neurons (AGRP-ChR2 mice; **Fig. 1a**). We tested the mice for optically evoked feeding behavior during the early light period, when mice normally eat little. Although AGRP neuron activity *in vivo* is unknown, optogenetic techniques can map the relationship between patterns of activity and behavior. We began by stimulating AGRP neurons with bursts of light pulses (20 Hz, 1 s) that were separated by 3 s and were repeated over 1 h (**Fig. 1b**). In brain-slice experiments, we found that a similar stimulation protocol could drive firing in AGRP neurons over extended timescales (**Supplementary Fig. 1**). This stimulus pattern is similar to activity patterns evoked in AGRP neurons by orexigenic hormones and neuropeptides applied to brain slices[20].

AGRP neurons are sufficient to induce voracious feeding

Within minutes, AGRP-ChR2 mice ate voraciously in response to photostimulation without training or prior exposure to the stimulus (**Fig. 1c**). Food intake was unchanged in photostimulated *agrp-cre* mice that were not infected with rAAV-FLEX-*rev*-ChR2:tdtomato (**Fig. 1c**). Because the stimulus was applied to well-fed mice during the early light period, these results indicate that AGRP neuron activity is not just permissive for feeding, but is instead sufficient to orchestrate feeding even under physiological, circadian and hypothalamic gene expression

Howard Hughes Medical Institute, Janelia Farm Research Campus, Ashburn, Virginia, USA. Correspondence should be addressed to S.M.S. (sternsons@janelia.hhmi.org).

Received 28 October 2010; accepted 16 December 2010; published online 5 January 2011; doi:10.1038/nn.2739

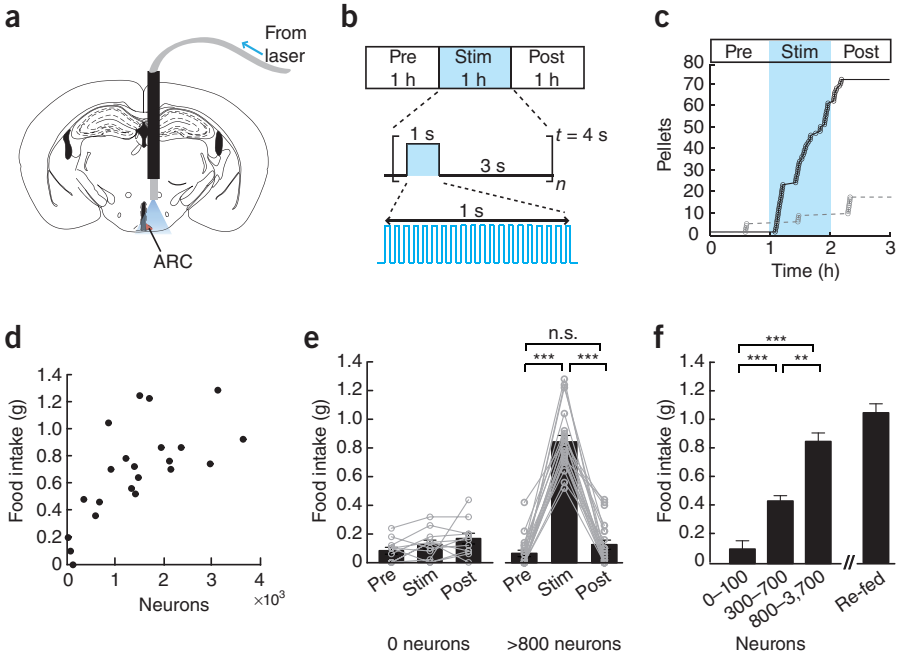

Figure 1 AGRP neurons are sufficient to evoke voracious food consumption in well-fed mice. (**a**) For light delivery, an optical fiber was implanted ~0.8 mm above the ARC (red). (**b**) Experimental design. Food intake was recorded before, during and after photostimulation. The stimulus was applied repeatedly over 1 s followed by a 3-s break. Photostimulation frequency was 20 Hz with 10-ms light pulses. (**c**) Photostimulation in an AGRP-ChR2 mouse (black) evoked voracious food consumption during the stimulation period, but not in a mouse without ChR2 expression (gray). (**d**) Food intake was dependent on the number of ChR2-expressing AGRP neurons. Circles represent 1 h of food intake for individual mice ($n = 22$). (**e**) Mice without ChR2 expression in AGRP neurons ($n = 11$) did not show a significant difference in food intake during photostimulation, whereas in mice with greater than 800 ChR2-expressing neurons ($n = 16$), the increase in food intake during photostimulation was significant. n.s., not significant ($P \geq 0.05$); $^{**}P < 0.01$, $^{***}P < 0.001$. Circles connected by lines represent food intake for individual mice. (**f**) Food intake during photostimulation was significantly increased in mice with intermediate (300–700 neurons, $n = 3$) or high levels of ChR2 expression (>800 neurons, $n = 16$) relative to mice with low or no ChR2 (0–100 neurons, $n = 14$). Photostimulation-induced food consumption was nearly as great as the magnitude of re-feeding ($n = 9$) for 1 h after 24 h of food deprivation. Error bars represent s.e.m.

conditions that are typically associated with satiety. However, it was unclear whether AGRP neurons serve simply as a switch for feeding behavior, in which case food intake would be expected to rise discontinuously following sufficient neuron activation. Alternatively, the intensity of feeding behavior could be closely tied to the level and duration of neuron activity, which would lead to a graded, continuous increase in feeding with increasing AGRP neuron activity. To address these possibilities, we investigated the relationship of externally imposed neuron activity to the magnitude and dynamics of the behavioral response.

The magnitude of food intake showed an increasing relationship with the number of ChR2-expressing neurons (**Fig. 1d**). In mice with zero or less than 100 ChR2-expressing neurons, no evoked feeding was observed (**Fig. 1e**). Photostimulated mice with 300–700 ChR2-expressing neurons consumed significantly more food ($P < 0.001$; **Fig. 1f**). For mice with more than 800 ChR2-expressing neurons, feeding responses were still greater and mice were effectively at maximal levels of consumption (for greater than 800 neurons, neurons versus food intake; linear least-squares goodness of fit, $r^2 = 0.06$). Furthermore, evoked food intake was nearly as large as re-feeding after 24 h of food deprivation (1-h intake; stimulated, 0.85 ± 0.06 g; re-fed after fasting, 1.04 ± 0.06 g; **Fig. 1f**). After photostimulation was terminated, feeding returned to pre-stimulus levels (**Fig. 1e**). Notably, consumption elicited by AGRP neuron activation was directed toward food and not water, which was freely available in the cage. All mice for which water consumption was recorded ate before drinking in response to photostimulation (12 of 12 mice) and drinking was not initiated until 13.0 ± 0.9 min after feeding started. Also, the feeding response magnitude did not appear to be related to a specific distribution of ChR2-expressing AGRP neurons along the rostral-caudal length on the ARC (**Supplementary Fig. 2**). Because feeding increased with the number of ChR2-expressing AGRP neurons (**Fig. 1f**), this indicates that AGRP neuron activity produces a signal to which there is a proportional and behaviorally specific food-directed response. To explore this further, we considered the effect of different AGRP neuron stimulation patterns.

Evoked feeding depends on photostimulus frequency

We tested the dependence of food intake on stimulus frequency using two protocols. On subsequent days, the stimulus frequency was varied between 20, 10 and 2 Hz, followed by a return to 20 Hz (stimulus protocol 1; **Fig. 2a**). Under these conditions, food intake during photostimulation was significantly increased relative to the pre-stimulus period (**Supplementary Fig. 3a–d**) and consumption diminished with decreasing stimulus frequency (**Fig. 2b**). Notably, for each mouse, feeding during the second 20-Hz stimulation trial was similar to the amount consumed in the initial trial despite variability in consumption across individual subjects (linear least-squares fit for consumption in trial 1 versus trial 2, slope = 0.81; $r^2 = 0.70$; **Supplementary Fig. 3e**), demonstrating that evoked food consumption is consistent across subsequent trials of AGRP neuron activation.

Because this protocol also reduced the number of light pulses in the brain as the stimulus frequency was decreased, we sought to distinguish whether these results were a result of the reduced number of photostimuli or if AGRP neuron–evoked food intake was frequency dependent. To test this, we delivered 20 light pulses every 10 s such that 20- and 2.5-Hz stimulation frequencies could be applied while maintaining the same number of stimuli over the 1-h stimulation epoch (stimulus protocol 2; **Fig. 2c**). In this case, consumption still decreased significantly with stimulation frequency ($P = 0.007$; **Fig. 2d**). Thus, bursts of AGRP neuron activity influence feeding behavior most effectively.

Dynamics of light-evoked feeding

Although AGRP neurons have been associated with long-term regulation of energy homeostasis, the rapid manipulation of neuron activity that we used allowed us to investigate the short-term dynamics of AGRP neuron–mediated feeding. The latency to food consumption with photostimulation of AGRP-ChR2 mice was dependent on the number of infected neurons (**Fig. 3a**). Mice with more than 800 ChR2-expressing AGRP neurons and no prior exposure to photostimulation showed an average latency to consumption of 6.1 ± 0.9 min (range: 1.9–13.8 min). Mice with intermediate numbers of ChR2-expressing neurons (300–700 neurons)

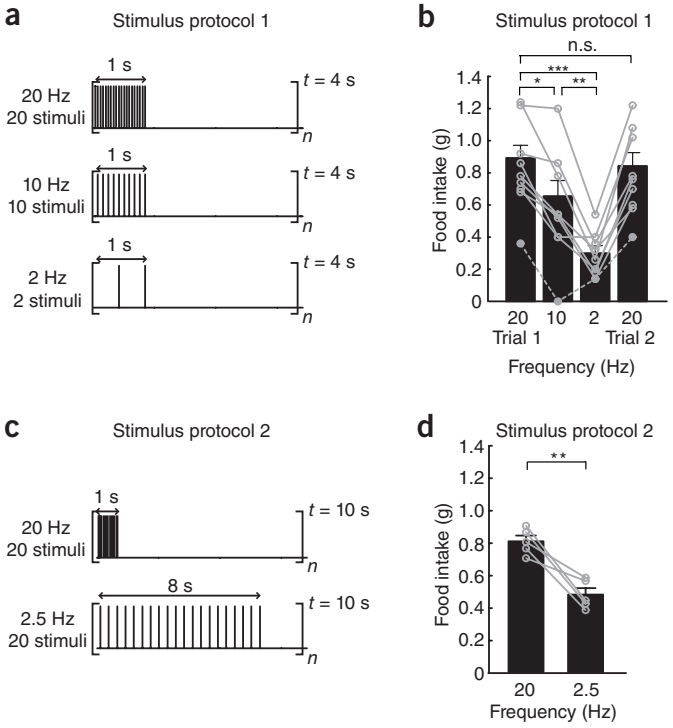

Figure 2 AGRP neuron–evoked feeding is dependent on the stimulation frequency. (**a**) Stimulus protocol 1. Bursts of light pulses were applied for 1 s followed by a 3-s break that repeated continuously for 1 h. In the burst, frequency (Hz) and number (pulses) was varied between 20, 10, 2 and 20 on successive days for AGRP-ChR2 mice. (**b**) Dependence of food intake on stimulation frequency (stimulus protocol 1) for mice with greater than 800 ChR2-expressing neurons ($n = 8$). As the stimulus frequency was reduced, feeding decreased. The gray dashed trace shows an example of a mouse with intermediate ChR2 expression (600 neurons, not included in sample mean) that had a similar relationship. On the final day, food intake was measured again in response to a second 20-Hz stimulation trial and was found to be similar to the consumption from the first day. Circles represent food intake for individual mice. n.s., not significant ($P \geq 0.05$); $^{*}P < 0.05$, $^{**}P < 0.01$, $^{***}P < 0.001$. (**c**) Stimulus protocol 2. Bursts of 20 light pulses were delivered every 10 s such that 20-Hz and 2.5-Hz stimulation frequencies could be applied while maintaining the same number of stimuli over the 1-h stimulation epoch. (**d**) Mice that received different stimulus frequencies (20 and 2.5 Hz), but the same total number of stimuli over 1 h (stimulus protocol 2), also showed a reduction in food intake with decreasing stimulus frequency ($n = 5$). Error bars represent s.e.m.

had substantially longer latencies to food consumption (33.6 ± 1.5 min), which is analogous to the moderate consumption observed in these mice. Once food intake was initiated, an early bout of avid feeding was typically followed by smaller bouts of various sizes (**Fig. 3b**). We calculated feeding bouts by analysis of the inter-pellet intervals (IPIs)[21,22] to determine a bout threshold (IPI_{thresh} = 2.4 min; see Online Methods and **Supplementary Figs. 4–6**), which showed that the mean duration of the first bout was 11.6 ± 0.8 min, during which 28.1 ± 1.6 food pellets were consumed. Bout termination has typically been attributed to the onset of short-term satiety cues[21], such as stomach distension or hormonal signals. Notably, most mice resumed food intake later during the photostimulation epoch, possibly reflecting a balance between AGRP neuron activity and satiety signals.

Because feeding is a complex behavior that involves motivational, sensory and motor circuits, we investigated whether AGRP neuron activity was only a trigger that initiates a self-propagating feeding response or if continuous photostimulation was required to sustain consumption. To test this, we measured the timescale over which food intake ceased after stimulation was terminated during the first feeding bout. Mice were photostimulated until 5 min after the first food pellet was taken, which is less than half of the average first bout duration for continuously stimulated mice. As expected, consumption was maintained throughout the stimulation period; however, first bout duration (7.3 ± 1.3 min; **Fig. 3c**), first bout consumption (18.3 ± 3.8 pellets; **Fig. 3d**) and total food consumption over 1 h (21.2 ± 4.0 pellets; **Fig. 3d**) were all significantly less than with continuous stimulation. In addition, in mice stimulated for only 5 min after taking the first pellet, total food consumption over 1 h was not significantly different ($P = 0.19$) than during the first bout, whereas in mice continuously stimulated for 1 h, total food intake was significantly greater ($P = 0.0011$) relative to the first bout, which is due to intake resulting from subsequent photostimulation-evoked bouts (**Fig. 3b**,**d**). These results indicate that AGRP neuron–evoked feeding behavior, once initiated, must be sustained by ongoing stimulation, and most mice (4 of 6) quickly stopped feeding after the offset of the stimulus. Nevertheless, we found that, even in this initial bout, the feeding was not strictly photostimulus bound. Food intake was proportional to the photostimulus, but, for some AGRP-ChR2 mice (2 of 6), consumption extended beyond the photostimulation for several minutes (**Supplementary Fig. 6**), indicating that the participation of efferent circuits sustaining food intake can continue for a short time after AGRP neuron stimulation is terminated.

Evoked feeding does not require melanocortin suppression

One downstream component of this circuit is POMC neurons, which are inhibited by AGRP neurons, and we sought to test whether suppression of POMC neuron–mediated melanocortin signaling was the means by which photostimulated AGRP neurons evoked feeding behavior. For this, we first examined whether activating POMC neurons was sufficient to reduce food intake. In brain-slice experiments, photostimulation of ChR2-expressing POMC neurons using protocol 1 (20 Hz) reliably drove POMC neuron firing (**Supplementary Fig. 7**). This stimulus, applied at the transition to the dark period in mice fed

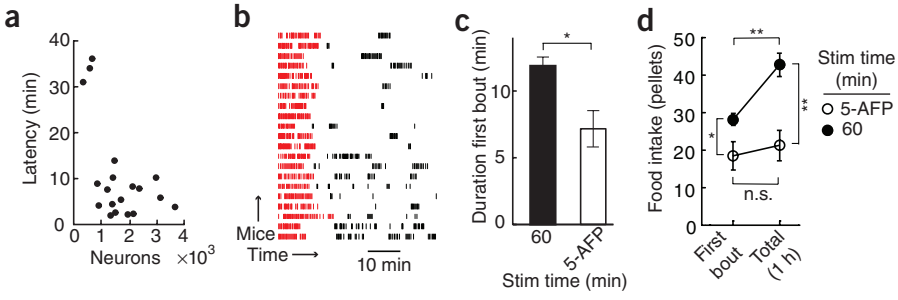

Figure 3 AGRP neuron–evoked feeding is rapidly initiated by stimulus onset and terminated after its offset. (**a**) Latency to food intake after photostimulation onset for each mouse (circles, $n = 19$). (**b**) For AGRP-ChR2 mice with greater than 800 ChR2-expressing neurons, the raster plot of food intake aligned to the first pellet shows an initial feeding bout (red ticks) and more variable subsequent bouts (black ticks). Each row is from an individual mouse. (**c**) The duration of the first bout during continuous photostimulation (filled bar, $n = 16$) was reduced when stimulation was terminated 5 min after the first pellet (AFP) was taken (empty bar, $n = 5$). $^{*}P < 0.05$. (**d**) Food intake for the first bout and over a 60-min period for mice continuously stimulated for 1 h (filled circles) and mice in which stimulation was terminated 5 min AFP (empty circles). n.s., not significant ($P \geq 0.05$); $^{**}P < 0.01$. Error bars represent s.e.m.

ad libitum (see Online Methods), did not significantly affect feeding over the 2 h straddling dark period onset (baseline, 0.32 ± 0.03 g; photostimulated, 0.26 ± 0.04; n = 9, paired t test, P = 0.30). However, applying this stimulus pattern for 24 h significantly reduced ($P < 0.001$) food intake by 39% (**Fig. 4a**) and body weight by 7% (**Fig. 4b**). Applying light pulses in *pomc-cre* mice lacking ChR2 expression did not significantly change food intake over 24 h (107%, $P = 0.43$; **Fig. 4c**). Furthermore, POMC neuron stimulation in A^y mice, in which the ectopically expressed *agouti* protein constitutively blocks melanocortin receptors[23], did not show reduced feeding (**Fig. 4d**); thus, POMC neuron–mediated hypophagia required melanocortin receptor signaling. Notably, this requirement for melanocortin receptor signaling indicates that other POMC neuron–derived neurotransmitters and neuropeptides, such as the anorexigenic peptide cocaine and amphetamine-related transcript[24,25], are not sufficient to reduce *ad libitum* food intake under these conditions.

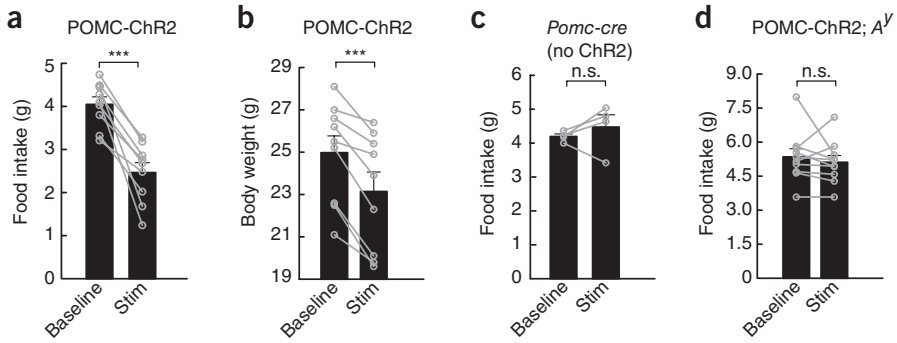

Figure 4 POMC neurons inhibit food intake and body weight through melanocortin receptors. (**a**,**b**) Photostimulation of POMC neurons (20 Hz, protocol 1 extended for 24 h) led to a reduction of food intake (**a**) and body weight (**b**) (n = 9). *** $P < 0.001$. (**c**) *Pomc-cre* mice without ChR2 expression in POMC neurons (n = 4) did not show a significant change in food intake over 24 h of photostimulation. n.s., not significant ($P \geq 0.05$). (**d**) In POMC-ChR2; A^y mice, hypophagia from POMC neuron activation was blocked by *agouti* antagonism of melanocortin signaling (n = 10). Baseline refers to average food intake or body weight for the 2 d before photostimulation. Error bars represent s.e.m.

Because POMC neurons required melanocortin signaling to induce hypophagia, which was completely blocked by the A^y mutation, we tested whether AGRP neuron–evoked food intake was a result of suppression of this POMC neuron–mediated pathway by stimulating AGRP neurons in A^y mice. In these mice, food intake was strongly activated in response to photostimulation (**Fig. 5**) and was similar to that observed in photostimulated AGRP-ChR2 mice (**Fig. 1e**). In addition, the latency to consumption of the first pellet was also comparable to response latencies in AGRP-ChR2 mice (6.2 ± 2.0 min, n = 7). These results complement the finding that anorexia from AGRP neuron ablation is not rescued by melanocortin blockade[13] and indicate that inhibition of melanocortin output by AGRP neurons is not a necessary condition for acutely evoked feeding behavior.

DISCUSSION

We explored the causal relationship between cell type–specific neuron activation and feeding behavior for AGRP and POMC neurons in the hypothalamic ARC. Our results indicate that simple stimulus patterns in AGRP neurons are sufficient to rapidly induce the animal to perform the complex behavioral sequences to seek and consume food. AGRP neuron stimulation was not simply a trigger for feeding; instead, we found that the level of AGRP neuron activity was integral to the magnitude, dynamics and duration of evoked feeding. Food consumption was greater and latency to eat decreased with increasing numbers of photoexcitable neurons. In addition, food intake was reduced as the stimulus frequency was decreased, consistent with a graded behavioral response to different neuron activities. Finally, continuation of evoked feeding required ongoing stimulation of AGRP neurons, which suggests that activity in downstream circuits is tied to AGRP neuron signaling during the behavior. Such measurements were not previously accessible without genetically encoded tools for cell type–specific, temporally precise manipulation of neuron activity. Together, these results indicate that there is a close relationship between AGRP neuron signaling and the downstream circuits that influence the diverse sensory, motor and motivational components that underlie this behavior.

Selective stimulation of POMC neurons gave the opposite behavioral outcome. Food intake and body weight were reduced over 24 h of continuous photostimulation, an effect that required signaling through melanocortin receptors. However, in contrast with pharmacological studies with acute application of melanocortin receptor agonists[26,27], POMC neuron stimulation for 2 h straddling dark period onset did not reduce food intake. This difference likely stems from the constraints associated with activation of intrinsic neurons as compared with intracranial injection of a neuromodulator. Specifically, the axon projections of a neuron and the natural expression level of an endogenous neuromodulator limit its distribution and the amount available to interact with downstream receptors. Another aspect of selective neuron activation is that it allows the contribution of other co-released substances to be measured. For POMC neurons, no effect on *ad libitum* feeding behavior was observed with melanocortin receptors blocked in A^y mice, indicating that co-released modulators and neurotransmitters were not sufficient to inhibit food intake under our experimental conditions.

Because the melanocortin pathway regulates feeding behavior, AGRP suppression of POMC-derived melanocortin signaling has been widely considered to be a pathway through which these neurons could rapidly increase feeding behavior[11]. However, although these cell populations interact, we found that inhibition of melanocortin receptors was not necessary for an acute AGRP neuron–evoked feeding response. Although these photostimulation results do not exclude a role for this pathway in the regulation of food intake over timescales longer than those that we investigated, they suggest that AGRP neurons are capable

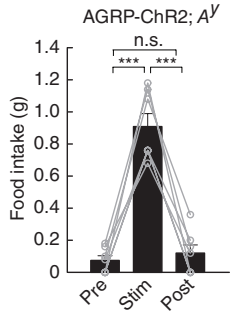

Figure 5 Evoked feeding does not require melanocortin suppression. Photostimulation of AGRP-ChR2; A^y mice evoked avid food intake, indicating that AGRP neurons can promote feeding independently of melanocortin receptor suppression (n = 7). n.s., not significant ($P \geq 0.05$); *** $P < 0.001$. Error bars represent s.e.m.

of independently engaging other downstream circuits that coordinate feeding. Future experiments could focus on the signaling pathways necessary for evoked feeding, which are likely mediated by other co-released components of AGRP neurons, such as the neuromodulator NPY and the fast neurotransmitter GABA[14].

A notable property of AGRP neurons was the capacity for simple photostimulus patterns to drive feeding behavior selectively without training or prior exposure to AGRP neuron stimulation. Previous studies have shown that simple activity patterns played into cortical neurons can be used to train a behavioral task or activate a learned behavior[28,29]. In other studies, stimulation of molecularly defined populations conditioned a place preference[30], reduced latency to waking[31] and elevated respiration[32]. However, the capability of a small molecularly defined neuron population to generate a goal-directed behavior without training has not, to the best of our knowledge, been previously described. One explanation for this result is that AGRP neurons have a dedicated role for controlling feeding behavior and that these exogenously applied activity patterns can substitute for patterns observed during normal activation of these neurons, for example, in a state of energy deficit. Although natural activity patterns in behaving animals are not known for AGRP neurons, optogenetic techniques allowed us to probe the capacity of these neurons and their downstream signaling pathways to influence feeding behavior and we found that a range of activity patterns were sufficient to activate a proportional feeding response.

Thus, these neurons, which transduce circulating signals of metabolic state such as leptin, ghrelin and glucose[33] into electrical activity, act as interoceptive sensory neurons that can control feeding behavior and may contribute to mediating the internal representation of hunger. Analogous to externally oriented sensory systems in which anatomical and functional properties of sensory neurons have facilitated the elucidation of neural pathways responsible for sensation and perception, the axon projections of AGRP neurons[34] may guide the identification of the motivational, hedonic and autonomic circuits that underlie control of feeding behavior. Because AGRP neurons also provide a genetically accessible entry point into these circuits, we propose that new genetically encoded tools for rapid manipulation of neuronal and synaptic function could be applied to dissect these discrete pathways under normal conditions, as well as in pathological states of over- and under-eating.

METHODS

Methods and any associated references are available in the online version of the paper at http://www.nature.com/natureneuroscience/.

Note: Supplementary information is available on the Nature Neuroscience website.

ACKNOWLEDGMENTS

We thank G. Shtengel for assistance with photostimulation equipment and software, R. Shusterman for assistance with data analysis, H. Peng for image analysis tools, J. Osborne and T. Tabachnik for equipment design and fabrication, A. Arnold for imaging support, B. Shields and A. Hu for histology support, and J. Cox for mouse breeding and genotyping support. K. Svoboda, G. Murphy, J. Dudman, A. Lee, and S.E.R. Egnor commented on the manuscript. This research was funded by the Howard Hughes Medical Institute.

AUTHOR CONTRIBUTIONS

Y.A. performed the behavioral experiments and D.A. performed and analyzed electrophysiological experiments. Y.A. and S.M.S. designed the study, analyzed the data and wrote the paper.

COMPETING FINANCIAL INTERESTS

The authors declare no competing financial interests.

Published online at http://www.nature.com/natureneuroscience/.
Reprints and permissions information is available online at http://www.nature.com/reprintsandpermissions/.

1. Morton, G.J., Cummings, D.E., Baskin, D.G., Barsh, G.S. & Schwartz, M.W. Central nervous system control of food intake and body weight. *Nature* **443**, 289–295 (2006).
2. Ollmann, M.M. *et al.* Antagonism of central melanocortin receptors in vitro and in vivo by agouti-related protein. *Science* **278**, 135–138 (1997).
3. Clark, J.T., Kalra, P.S., Crowley, W.R. & Kalra, S.P. Neuropeptide Y and human pancreatic polypeptide stimulate feeding behavior in rats. *Endocrinology* **115**, 427–429 (1984).
4. Levine, A.S. & Morley, J.E. Neuropeptide Y: a potent inducer of consummatory behavior in rats. *Peptides* **5**, 1025–1029 (1984).
5. Stanley, B.G. & Leibowitz, S.F. Neuropeptide Y: stimulation of feeding and drinking by injection into the paraventricular nucleus. *Life Sci.* **35**, 2635–2642 (1984).
6. Takahashi, K.A. & Cone, R.D. Fasting induces a large, leptin-dependent increase in the intrinsic action potential frequency of orexigenic arcuate nucleus neuropeptide Y/Agouti-related protein neurons. *Endocrinology* **146**, 1043–1047 (2005).
7. Tsujii, S. & Bray, G.A. Acetylation alters the feeding response to MSH and beta-endorphin. *Brain Res. Bull.* **23**, 165–169 (1989).
8. Yaswen, L., Diehl, N., Brennan, M.B. & Hochgeschwender, U. Obesity in the mouse model of pro-opiomelanocortin deficiency responds to peripheral melanocortin. *Nat. Med.* **5**, 1066–1070 (1999).
9. Cowley, M.A. *et al.* Leptin activates anorexigenic POMC neurons through a neural network in the arcuate nucleus. *Nature* **411**, 480–484 (2001).
10. Roseberry, A.G., Liu, H., Jackson, A.C., Cai, X. & Friedman, J.M. Neuropeptide Y-mediated inhibition of proopiomelanocortin neurons in the arcuate nucleus shows enhanced desensitization in ob/ob mice. *Neuron* **41**, 711–722 (2004).
11. Cowley, M.A. *et al.* Electrophysiological actions of peripheral hormones on melanocortin neurons. *Ann. NY Acad. Sci.* **994**, 175–186 (2003).
12. Luquet, S., Perez, F.A., Hnasko, T.S. & Palmiter, R.D. NPY/AgRP neurons are essential for feeding in adult mice but can be ablated in neonates. *Science* **310**, 683–685 (2005).
13. Wu, Q., Howell, M.P., Cowley, M.A. & Palmiter, R.D. Starvation after AgRP neuron ablation is independent of melanocortin signaling. *Proc. Natl. Acad. Sci. USA* **105**, 2687–2692 (2008).
14. Wu, Q., Boyle, M.P. & Palmiter, R.D. Loss of GABAergic signaling by AgRP neurons to the parabrachial nucleus leads to starvation. *Cell* **137**, 1225–1234 (2009).
15. Boyden, E.S., Zhang, F., Bamberg, E., Nagel, G. & Deisseroth, K. Millisecond-timescale, genetically targeted optical control of neural activity. *Nat. Neurosci.* **8**, 1263–1268 (2005).
16. Li, X. *et al.* Fast noninvasive activation and inhibition of neural and network activity by vertebrate rhodopsin and green algae channelrhodopsin. *Proc. Natl. Acad. Sci. USA* **102**, 17816–17821 (2005).
17. Atasoy, D., Aponte, Y., Su, H.H. & Sternson, S.M.A. FLEX switch targets Channelrhodopsin-2 to multiple cell types for imaging and long-range circuit mapping. *J. Neurosci.* **28**, 7025–7030 (2008).
18. Kaelin, C.B., Xu, A.W., Lu, X.Y. & Barsh, G.S. Transcriptional regulation of agouti-related protein (Agrp) in transgenic mice. *Endocrinology* **145**, 5798–5806 (2004).
19. Balthasar, N. *et al.* Leptin receptor signaling in POMC neurons is required for normal body weight homeostasis. *Neuron* **42**, 983–991 (2004).
20. van den Top, M., Lee, K., Whyment, A.D., Blanks, A.M. & Spanswick, D. Orexigen-sensitive NPY/AgRP pacemaker neurons in the hypothalamic arcuate nucleus. *Nat. Neurosci.* **7**, 493–494 (2004).
21. Tolkamp, B.J., Allcroft, D.J., Austin, E.J., Nielsen, B.L. & Kyriazakis, I.I. Satiety splits feeding behaviour into bouts. *J. Theor. Biol.* **194**, 235–250 (1998).
22. Tolkamp, B.J. & Kyriazakis, I.I. To split behaviour into bouts, log-transform the intervals. *Anim. Behav.* **57**, 807–817 (1999).
23. Miller, M.W. *et al.* Cloning of the mouse agouti gene predicts a secreted protein ubiquitously expressed in mice carrying the lethal yellow mutation. *Genes Dev.* **7**, 454–467 (1993).
24. Kristensen, P. *et al.* Hypothalamic CART is a new anorectic peptide regulated by leptin. *Nature* **393**, 72–76 (1998).
25. Elias, C.F. *et al.* Leptin activates hypothalamic CART neurons projecting to the spinal cord. *Neuron* **21**, 1375–1385 (1998).
26. Rossi, M. *et al.* A C-terminal fragment of Agouti-related protein increases feeding and antagonizes the effect of alpha-melanocyte stimulating hormone in vivo. *Endocrinology* **139**, 4428–4431 (1998).
27. Fan, W., Boston, B.A., Kesterson, R.A., Hruby, V.J. & Cone, R.D. Role of melanocortinergic neurons in feeding and the agouti obesity syndrome. *Nature* **385**, 165–168 (1997).
28. Huber, D. *et al.* Sparse optical microstimulation in barrel cortex drives learned behaviour in freely moving mice. *Nature* **451**, 61–64 (2008).
29. Houweling, A.R. & Brecht, M. Behavioural report of single neuron stimulation in somatosensory cortex. *Nature* **451**, 65–68 (2008).
30. Tsai, H.C. *et al.* Phasic firing in dopaminergic neurons is sufficient for behavioral conditioning. *Science* **324**, 1080–1084 (2009).
31. Adamantidis, A.R., Zhang, F., Aravanis, A.M., Deisseroth, K. & de Lecea, L. Neural substrates of awakening probed with optogenetic control of hypocretin neurons. *Nature* **450**, 420–424 (2007).
32. Abbott, S.B. *et al.* Photostimulation of retrotrapezoid nucleus phox2b-expressing neurons *in vivo* produces long-lasting activation of breathing in rats. *J. Neurosci.* **29**, 5806–5819 (2009).
33. Belgardt, B.F., Okamura, T. & Bruning, J.C. Hormone and glucose signaling in POMC and AgRP neurons. *J. Physiol. (Lond.)* **587**, 5305–5314 (2009).
34. Broberger, C., Johansen, J., Johansson, C., Schalling, M. & Hokfelt, T. The neuropeptide Y/agouti gene-related protein (AGRP) brain circuitry in normal, anorectic, and monosodium glutamate-treated mice. *Proc. Natl. Acad. Sci. USA* **95**, 15043–15048 (1998).

ONLINE METHODS

Animals. All experimental protocols were conducted according to US National Institutes of Health guidelines for animal research and were approved by the Institutional Animal Care and Use Committee at Janelia Farm Research Campus. *Agrp-cre*[18] and *pomc-cre*[19] mice have been described previously. *Agrp-cre; A^y* and *pomc-cre; A^y* mice were generated by crossing *agrp-cre* and *pomc-cre* mice, respectively, with heterozygous *A^y* mice (Jackson Laboratories). Mice were genotyped for *cre* (Transnetyx) and *A^y* mice were identified by their yellow coat color. Typically, male mice were used. Females were occasionally used for experiments involving *agrp-cre; A^y* (2 of 7 mice) and *pomc-cre; A^y* (3 of 10 mice); their behavioral responses were not different from results with male mice.

Stereotaxic viral delivery and fiber guide system implantation. Mice were anesthetized with isoflurane and were placed into a stereotaxic apparatus (David Kopf Instruments). The skull was exposed via a small incision and a small hole was drilled for injection and fiber guide cannula placement. Mice were injected with virus on only one side of the brain. A pulled glass pipette with 20–40-μm tip diameter was inserted into the brain and two unilateral injections (60 nl) of the rAAV2/rh10-FLEX-*rev*-ChR2:tdTomato virus (titer: 1.1×10^{13} genomic copies per ml, University of Pennsylvania Gene Therapy Program Vector Core; rAAV2-FLEX-*rev*-ChR2:tdTomato plasmid is available from www.addgene.com, plasmid 18917) were made at coordinates around the ARC (bregma, –1.2 mm; midline, +0.2 mm; dorsal surface, –5.85 mm and –5.7 mm). A micromanipulator (Narishige) was used to control the injection speed (30 nl min^{-1}) and the pipette was withdrawn 15 min after the final injection. This was followed by insertion of a guide cannula (4.5 mm, 26GA, Plastics One) through the craniotomy. Grip cement (DENTSPLY) was used to anchor the guide cannula to the skull and a dummy cannula (33GA, Plastics One) was inserted to keep the fiber guide from becoming clogged. Mice were returned to their home cage typically for 10–14 d to recover and for expression of ChR2:tdtomato.

Components for food consumption and photostimulation. In the home cage, mice had *ad libitum* access to mouse chow (PicoLab Rodent Diet 20, 5053 tablet, TestDiet). For behavioral testing, mice were transferred into feeding cages (Coulbourn Instruments) and supplied with food pellets (20 mg each) of identical composition to the food in the home cage, delivered by an automatic pellet dispenser. Pellet removal was sensed by the offset of a beam break and an additional pellet was administered after a delay (10 s). Food consumption was monitored continuously by computer using Graphic State (Coulbourn Instruments). Mice also had water available *ad libitum* during behavioral experiments, which, in some cases, was monitored by optical detection (Coulbourn Instruments) of licks emitted toward the drinking spout. The mice were allowed to acclimate for 3 d before initiating the photostimulation protocols.

Light was delivered to the brain through an optical fiber. For positioning the fiber, mice were anesthetized with isoflurane the day before photostimulation and the tip (200-μm diameter core; BFH48-200-Multimode, NA 0.48; Thorlabs) was implanted through the fiber guide to a distance of ~0.8 mm from the ARC. The relationship of light scattering and absorption in the brain as a function of distance has been described previously[35]. Using this relationship, the light power exiting the fiber tip (10 mW) was estimated to correspond to 2.0 mW mm^{-2} at the ARC, which was sufficient to drive a behavioral response.

For optical delivery of light pulses with millisecond precision to multiple mice, the output from a 200-mW diode laser (Ciel 473 nm, Laser Quantum) was split into four beams using a combination of 50/50 beam splitters and turning mirrors (Thorlabs). Each beam was controlled using an acousto-optic modulator (AOM) (Quanta Tech, OPTO-ELECTRONIC) to generate light pulses that were launched into separate fiber ports (PAF-X-7, Thorlabs) and their corresponding optical fibers. Using these components, four mice could be simultaneously and independently photostimulated. The controlling software for the AOMs was written in LabView (National Instruments).

Behavioral experiments. AGRP-ChR2 and AGRP-ChR2; *A^y* mice were tested for evoked feeding behavior during the early light period (lights on at 6:00 a.m.). Food intake was recorded during a pre-stimulus baseline from 8:00 to 9:00 a.m., followed by a 1-h photostimulation period from 9:00 to 10:00 a.m. Afterwards, a post-stimulus period from 10:00 to 11:00 a.m. was also recorded. The primary photostimulation protocol consisted of light pulses (10 ms) for 1 s (20, 10, or 2 Hz) followed by a 3-s break, with the sequence repeating for 1 h.

We also used a second protocol in which the number of light pulses was kept constant for different stimulation frequencies. Here, 20 light pulses (10 ms each) were delivered for 1 or 8 s (20 or 2.5 Hz), respectively, and the sequence repeated every 10 s for 1 h.

POMC-ChR2 and POMC-ChR2; *A^y* mice were also tested for evoked feeding behavior. The photostimulation was initiated 1 h before the onset of the dark period and followed protocol 1 (20 Hz). Stimulation was sustained for 24 h because an acute reduction of food intake was not typically observed in these mice. Changes in food intake and body weight are reported relative to the mean values over 2 d before photostimulation.

Histology, imaging and neuron counting. After removing the optical fiber, mice were deeply anesthetized and then killed by perfusion with saline followed by 4% paraformaldehyde in phosphate buffered saline and fixed overnight in paraformaldehyde and transferred to phosphate buffered saline. Brain sections (50 μm) were cut by vibratome sectioning, mounted on glass slides using VECTASHIELD mounting medium with DAPI, and coverslipped for imaging. Neuron images were collected by confocal microscopy (Carl Zeiss) using tdtomato fluorescence. Neurons with red fluorescence were counted manually using V3D, an image visualization and analysis software[36]. Ambercrombie's correction[37] was applied to the neuron counts (slice thickness, 50 μm; AGRP neuron diameter, 14 ± 1 μm; correction factor, 0.78). In the text, neuron counts were rounded to the nearest hundred.

Electrophysiology. Experimental techniques were similar to those reported previously[17], and only the differences are described here. After viral infection (14-d incubation, viral injection between in postnatal day 21–25 mice) mice were deeply anesthetized with isoflurane and decapitated. Coronal brain slices containing the ARC were prepared in chilled cutting solution containing 234 mM sucrose, 28 mM $NaHCO_3$, 7 mM dextrose, 2.5 mM KCl, 7 mM $MgCl_2$, 0.5 mM $CaCl_2$, 1 mM sodium ascorbate, 3 mM sodium pyruvate and 1.25 mM NaH_2PO_4, aerated with 95% O_2/5% CO_2. Slices were transferred to artificial cerebrospinal fluid containing 119 mM NaCl, 25 mM $NaHCO_3$, 11 mM D-glucose, 2.5 mM KCl, 1.25 mM $MgCl_2$, 2 mM $CaCl_2$ and 1.25 mM NaH_2PO_4, aerated with 95% O_2/5% CO_2. Slices were incubated at 34 °C for 30 min and then maintained and recorded from at 20–24 °C. Neurons were identified and targeted by tdtomato fluorescence emission (excitation, 575 nm; emission, 640 nm; dichroic, 610 nm longpass; Chroma). Loose-seal, cell attached recordings (seal resistance, 20–70 MΩ) in the voltage-clamp recording mode with holding current maintained at zero were made using electrodes with tip resistances 4–5 MΩ filled with artificial cerebrospinal fluid. At the end of some recordings, tetrodotoxin (1 μM) was added to the bath to confirm that the responses were the results of voltage-gated sodium channels.

Photostimulation in brain slices. A laser (473 nm, CrystaLaser) was used to deliver light pulses at 0.1 mW. Light pulse duration (10 ms) was controlled by a Pockels cell (ConOptics) and a mechanical shutter (Vincent Associates). A focal spot was targeted onto the specimen with two x-y scanning mirrors (Cambridge Technology) through a 63× microscope objective (Olympus). Laser power was monitored with a photodiode for each light pulse. Neurons were repetitively stimulated for 30 min with bursts of 20 pulses over 1 s followed by either a 2-s (AGRP neurons) or a 3-s (POMC neurons) break. Because 10-ms pulses were used, the possibility existed for two action currents from a single light pulse. This was only observed for 0.073 ± 0.005% of the total light pulses in AGRP neurons and 0.66 ± 0.007% of the total light pulses in POMC neurons.

Electrophysiological analysis. Spikes were detected in a 15-ms window following each photostimulus using the template matching feature in Clampfit (Molecular Devices). The resulting annotations were visually inspected to confirm correct detection.

Analysis of feeding bouts resulting from photostimulation. We observed that photostimulation-evoked feeding consisted of at least three components occurring on different timescales. The first component was a rapid and regular consumption of pellets. The second component included short interruptions in feeding resulting from consumption of water or brief investigation of a distractor, after which mice would return to regular food consumption. The third timescale was the intervals during which the animal would rest or groom and pay little

attention to food. Here, we calculated feeding bouts to include the first two components. Inter-pellet intervals (IPIs) were log-transformed for all AGRP-ChR2 mice with greater than 800 ChR2-expressing AGRP neurons. The frequency distribution of log(IPIs) was fit to a double log-normal model[22] (**Supplementary Fig. 4**)

$$y = A_1 e^{\frac{-(t-\mu_1)^2}{2\sigma_1^2}} + A_2 e^{\frac{-(t-\mu_2)^2}{2\sigma_2^2}} \quad (1)$$

where y is the frequency distribution of log-transformed intervals with length t, μ_1 and μ_2 are the mean log(IPIs) of the two IPI groups, σ_1 and σ_2 are the s.d. of the two IPI groups, and A_1 and A_2 reflect the modeled peak frequencies of the two IPI components.

A threshold value for a feeding bout was calculated

$$\text{threshold} = \text{antilog}(\mu_2 + 3\sigma_2) \quad (2)$$

Bout duration and consumption were determined by applying this threshold (2.4 min) to the photostimulation-evoked food consumption curves for individual AGRP-ChR2 mice. Inspection of the bouts with respect to IPIs showed that the thresholding approach produced meaningful bouts for 1-h continuous stimulation (**Supplementary Fig. 5**), as well as for stimulation that was ceased only 5 min after the first pellet was taken (**Supplementary Fig. 6**). Bout duration was the time from the consumption of the first pellet to the last pellet with IPI < threshold and bout consumption was the number of pellets consumed for each animal over this time.

Statistical analysis. Values are reported as mean ± s.e.m. and error bars are s.e.m. Linear and nonlinear curve fitting was performed using the Curve Fitting Toolbox in Matlab (Mathworks). Statistical tests were paired (for all within subjects comparisons) or unpaired (for all between subjects comparisons) t tests and multiple comparisons were corrected by Holm's method[38].

35. Aravanis, A.M. *et al.* An optical neural interface: in vivo control of rodent motor cortex with integrated fiberoptic and optogenetic technology. *J. Neural Eng.* **4**, S143–S156 (2007).
36. Peng, H., Ruan, Z., Long, F., Simpson, J.H. & Myers, E.W. V3D enables real-time 3D visualization and quantitative analysis of large-scale biological image data sets. *Nat. Biotechnol.* **28**, 348–353 (2010).
37. Abercrombie, M. Estimation of nuclear population from microtome sections. *Anat. Rec.* **94**, 239–247 (1946).
38. Holm, S.A. A simple sequentially rejective multiple test procedure. *Scand. J. Stat.* **6**, 65–70 (1979).

doi:10.1038/nn.2739